The Plant Cell, Vol. 18, 612–625, March 2006, www.plantcell.org © 2006 American Society of Plant Biologists

PLASTOCHRON2 Regulates Leaf Initiation and Maturation in Rice [W]

Taiji Kawakatsu,[a] Jun-Ichi Itoh,[a] Kazumaru Miyoshi,[a] Nori Kurata,[b] Nena Alvarez,[c] Bruce Veit,[c] and Yasuo Nagato[a,1]

[a] Graduate School of Agricultural and Life Sciences, University of Tokyo, Tokyo 113-8657, Japan
[b] National Institute of Genetics, Mishima 411-8540, Japan
[c] AgResearch, Private Bag 11008, Palmerston North, New Zealand

In higher plants, leaves initiate in constant spatial and temporal patterns. Although the pattern of leaf initiation is a key element of plant shoot architecture, little is known about how the time interval between initiation events, termed plastochron, is regulated. Here, we present a detailed analysis of *plastochron2* (*pla2*), a rice (*Oryza sativa*) mutant that exhibits shortened plastochron and precocious maturation of leaves during the vegetative phase and ectopic shoot formation during the reproductive phase. The corresponding *PLA2* gene is revealed to be an orthologue of *terminal ear1*, a maize (*Zea mays*) gene that encodes a MEI2-like RNA binding protein. *PLA2* is expressed predominantly in young leaf primordia. We show that *PLA2* normally acts to retard the rate of leaf maturation but does so independently of *PLA1*, which encodes a member of the P450 family. Based on these analyses, we propose a model in which plastochron is determined by signals from immature leaves that act non-cell-autonomously in the shoot apical meristem to inhibit the initiation of new leaves.

INTRODUCTION

The arrangement of leaves and branches constitutes a major component of plant architecture. Since branches are formed in the axils of leaves, the pattern of leaf initiation has special significance. Leaves are generated from the shoot apical meristem (SAM) in constant spatial (phyllotaxy) and temporal (plastochron) patterns. Thus, knowledge of the regulatory mechanisms of plastochron and phyllotaxy would greatly enhance our understanding of plant architecture. To date, however, neither of these traits has been thoroughly analyzed.

Changes in the timing and the rate of developmental programs, known as heterochrony, can lead to significant morphological changes in organisms and play an important role in evolution (Gould, 1977). In plants, the mechanism of heterochrony or temporal regulation of development is poorly understood, although genes have been identified in several plant species that regulate juvenile–adult phase change (Poethig, 1988; Telfer and Poethig, 1998; Asai et al., 2002). With respect to plastochron, several genes have been identified: *PLASTOCHRON1* (*PLA1*) in rice (*Oryza sativa*; Miyoshi et al., 2004), *terminal ear1* (*te1*) in maize (*Zea mays*; Veit et al., 1998), and *ALTERED MERISTEM PROGRAM1* (*AMP1*), *PHYTOCHROME B* (*PHYB*), and *SERRATE* (*SE*) in *Arabidopsis thaliana* (Reed et al., 1993; Helliwell et al., 2001; Prigge and Wagner, 2001). *pla1*, *te1*, and *amp1* show shorter plastochron. By contrast, *phyB* and *se* show longer plastochron than the wild type. With each of these genes encoding a distinct class of protein and showing distinct loss-of-function phenotypes, the regulation of plastochron appears complex.

Regulation of phyllotaxy is to some degree independent of plastochron because some plastochron mutants do not exhibit phyllotactic change (Itoh et al., 1998). However, the normal initiation of a leaf primordium requires simultaneous determination of its position and timing. In addition, *te1* shows both shortened plastochron and, to a lesser extent, abnormal phyllotaxy (Veit et al., 1998). Accordingly, plastochron and phyllotaxy appear to depend, at least in part, on a common regulatory mechanism.

Two general types of models have been proposed for explaining phyllotactic pattern. The first model, referred to as the inhibitor model (reviewed in Steeves and Sussex, 1989), proposes that existing primordia produce a diffusible inhibitor of leaf formation and that the new primordium can only be initiated at the position where the inhibitor concentration is at a minimum. This model is supported by surgical experiments, in which incisions that separated newly formed leaf primordia from leaf-forming regions of the apex shifted the position of leaf formation toward preexisting leaves (Snow and Snow, 1931). The second model, termed the biophysical model, proposes that physical forces determine phyllotaxy (Green, 1985). This model has received support from experiments in which treatment with expansin, which normally acts to allow cell wall expansion, altered phyllotaxy (Fleming et al., 1997; Pien et al., 2001).

Recently, the auxin transport model has been developed based on the gradients of this plant hormone that are presumed to exist in the shoot apex and the effects that artificial manipulation of auxin levels have on leaf initiation. In this model, each

[1] To whom correspondence should be addressed. E-mail anagato@mail.ecc.u-tokyo.ac.jp; fax 81-3-5841-5063.
The author responsible for distribution of materials integral to the findings presented in this article in accordance with the policy described in the Instructions for Authors (www.plantcell.org) is: Yasuo Nagato (anagato@mail.ecc.u-tokyo.ac.jp).
[W] Online version contains Web-only data.
Article, publication date, and citation information can be found at www.plantcell.org/cgi/doi/10.1105/tpc.105.037622.

leaf primordium arises at a position where the auxin flows from surrounding regions to create a local concentration maximum (Reinhardt et al., 2000, 2003). Subsequently, the primordium functions as a sink for auxin, thereby depleting auxin from surrounding cells. This model can be considered to be a type of inhibitory field model, since newly formed leaves would inhibit leaf initiation in the neighboring region by reducing auxin content below a critical threshold.

A recent study showed that cytokinin is also involved in phyllotaxy. Maize *abphyl1* (*abph1*) encodes a cytokinin-inducible A-type response regulator, which is thought to act as a negative feedback regulator of cytokinin signaling (Giulini et al., 2004). *abphl1* mutations change the normal alternate phyllotaxy (leaves initiated singly on alternate sides of the shoot) to a decussate pattern (successive pairs of leaves initiated at 90° with respect to each other) (Jackson and Hake, 1999). This suggests that cytokinin signaling is involved in leaf initiation through some form of crosstalk with auxin signaling pathways.

As previously discussed, three types of genes whose recessive mutations cause shortened plastochron, including rice *PLA1*, maize *te1*, and *Arabidopsis AMP1* have been cloned (Chaudhury et al., 1993; Itoh et al., 1998; Veit et al., 1998; Helliwell et al., 2001; Miyoshi et al., 2004). The loss-of-function mutant *pla1* shows shortened plastochron and conversion of rachis branches to vegetative shoots, but the phyllotaxy is not modified. *pla1* plants have an enlarged SAM that is associated with more frequent cell divisions (Itoh et al., 1998), suggesting that cell division rate may influence plastochron. Supporting this hypothesis, transgenic tobacco (*Nicotiana tabacum*) plants constitutively expressing *cyclin* D showed an accelerated rate of cell division and shortened plastochron (Cockcroft et al., 2000). *PLA1* encodes a member of the plant-specific subfamily of cytochrome P450 monooxygenases and is expressed in young leaf primordia but not in the SAM (Miyoshi et al., 2004). This suggests that signals from leaf primordia can act non-cell-autonomously to regulate leaf initiation in the SAM. *te1* and *amp1* show shortened plastochron and abnormal phyllotaxy (Chaudhury et al., 1993; Veit et al., 1998) but not the heterochrony in the reproductive phase observed in *pla1. te1* encodes RNA binding protein, while *AMP1* encodes Glu carboxypeptidase (Veit et al., 1998; Helliwell et al., 2001). *te1* transcripts can be seen in the SAM and young leaf primordia, while *AMP1* is expressed in all organs. How these three genes might influence plastochron remains unclear.

We recently isolated several new mutant alleles of a rice gene, termed *PLA2*, which show shortened plastochron and the conversion of inflorescence branches to vegetative structures. In this article, we describe phenotypes of *pla2*, the genetic relationship between *PLA2* and *PLA1*, and molecular identification of *PLA2*. Double mutant phenotypes suggest that *PLA2* and *PLA1* act independently. By positional cloning, we show that *PLA2* encodes MEI2-like RNA binding protein that is likely to be a rice orthologue of *te1*. Interestingly, despite their similarity, *pla2* and *te1* show distinct phenotypes, suggesting that differences in the activities of the normal genes may be partly responsible for differences between the shoot architectures of rice and maize. Detailed analyses indicate that the primary function of *PLA2* resides in regulating leaf maturation, which in turn plays a major role in regulating plastochron in rice.

RESULTS

Phenotypes of *pla2* Mutants

Plastochron and Leaf Size

Rice plants normally initiate leaves from the SAM at regular intervals in 1/2 alternate phyllotaxy and, like many grasses, form several juvenile leaves in embryo before dormancy. In both the wild type and *pla2*, three leaves were present in mature embryos. After germination, both *pla2-1* and *pla2-2* showed an increased rate of leaf emergence compared with the wild type (Figures 1A and 1C). Since mature wild-type and *pla2* embryos have the same number of leaf primordia, the more frequent leaf emergence indicates a shorter plastochron for subsequently formed leaves in the *pla2* mutant. Given the similarity of *pla2-1* and

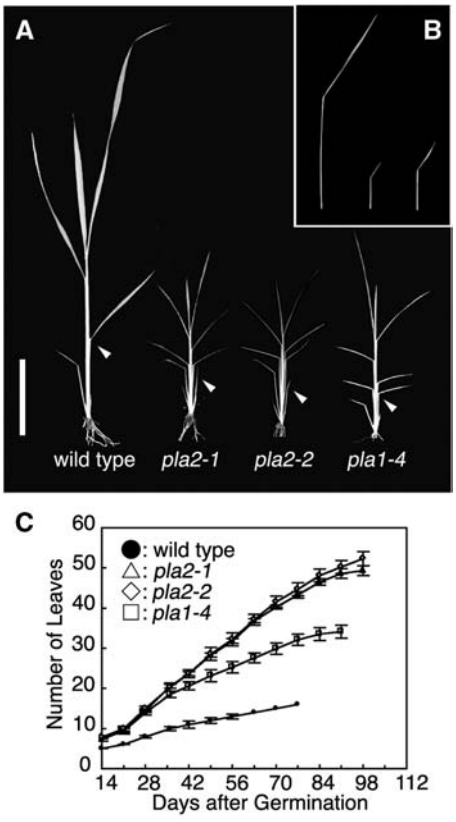

Figure 1. Vegetative Phenotypes of Wild-Type, *pla2*, and *pla1* Plants.

(A) Seedlings at 2 weeks after germination. The lamina joint of the third leaf does not bend in *pla2-1* and *pla2-2*, although they do bend in the wild type and *pla1-4.* Arrowheads indicate the lamina joints of the third leaf. Bar = 5 cm.

(B) Phenotype of the last vegetative leaf (flag leaf) of the wild type, *pla2-1*, and *pla1-4* from left to right. Leaf size is reduced strongly in *pla2-1* and *pla1-4.*

(C) Increase in the number of emerged leaves during development. Closed circles, open triangles, open diamonds, and open squares represent the wild type, *pla2-1*, *pla2-2*, and *pla1-4*, respectively. Bars indicate ± SD.

pla2-2 phenotypes, we chose to focus on *pla2-1* in this article. Plastochrons of the wild type and *pla2-1* were nearly constant throughout the vegetative phase at 5.0 and 1.8 d, respectively (Figure 1C). For comparison, we examined phenotypes of *pla1* mutants, which were reported previously (Itoh et al., 1998; Miyoshi et al., 2004). The plastochron of *pla2* is significantly shorter than *pla1* (1.8 versus 2.3). Furthermore, in contrast with *pla1*, in which the angle between the blade and sheath is increased for all leaves, the third leaf of *pla2* appears erect due to an irregular blade-sheath boundary (see Supplemental Figure 1 online). The transition of vegetative to reproductive phase was also delayed in *pla2-1* and *pla2-2.* Together with an extended vegetative period, *pla2* produced threefold as many leaves as the wild type (49 versus 16 leaves). Assuming that this increase reflects loss of normal *PLA2* function, these results suggest that the *PLA2* gene normally acts to inhibit leaf initiation. In addition to a shortened plastochron, *pla2* plants exhibited significantly smaller leaves than the wild type with respect to the length of blade and sheath and also the width of leaf blade (Figure 1B; see Supplemental Figures 2A to 2C online). As the size of epidermal cells of the third leaf in *pla2* was almost comparable to that in the wild type, this size reduction was exclusively due to the reduction in the number of cells (see Supplemental Figure 3 online). The possibility of a causal relationship between leaf size and plastochron is reinforced by the phenotype of *pla1*, which also shows reduced leaf size and plastochron but not as severe as seen for *pla2* (Figure 1B; see Supplemental Figures 2A to 2C online). Thus, there exists a positive correlation between plastochron and leaf size in the wild type, *pla1*, and *pla2*.

Precocious Maturation of pla2 Leaves

To elucidate the function of *PLA2* in leaves, we compared the timing of developmental landmarks for the leaves of wild-type and *pla2* plants. To represent different leaves, we used a plastochron numbering (PN) system; P1 represents the youngest primordium, P2 the next youngest, etc. (Itoh et al., 2005). P0 is defined as founder cell stage, which immediately precedes appearance of the primordium bulge on the SAM. In wild-type plants, a series of developmental events can be related to specific PNs. Since the sequence of development for the leaf has been described in detail previously (Itoh et al., 2005), only major events are outlined here. Cells at the P0 stage are recruited as leaf founder cells, an event marked by downregulation of *O. sativa HOMEOBOX1* (*OSH1*) (Figures 2A and 2I). *OSH1* is a rice orthologue of maize *KNOTTED1* and is expressed in indeterminate cells (Sato et al., 1996). At this stage, *O. sativa PNH1*, which is a homologue of *Arabidopsis PINHEAD/ZWILL* and is expressed in the developing vascular bundles and presumptive regions of bundle sheath, is expressed first (Figures 2C and 2I; Nishimura et al., 2002). This expression lasts until P4 stage. Two margins of the leaf primordium overlap and enclose the SAM at P2 stage (Figures 2E and 2I). At this stage, vascular bundles become visible (Figures 2E and 2I). Formation of vascular bundles continues until P5 (Figures 2C and 2I). A protrusion marking the ligule primordium appears at P3 at the boundary between leaf blade and sheath on the adaxial side (Figures 2G and 2I). After differentiation of the ligule primordium, the leaf blade elongates rapidly. This continues from P4 to P5 (Figure 2I). When the leaf blade has nearly stopped elongating, the more basal leaf sheath starts to elongate rapidly until it reaches P6 (Figure 2I). After the leaf sheath elongation has finished, the leaf blade bends away from the shoot axis at its junction with the leaf sheath. At P5, lacunae (air spaces) are formed (Figures 2C and 2I).

In *pla2-1*, leaves exhibited a normal sequence of PN-related development (Figures 2B, 2D, 2F, 2H, and 2I), except that leaf sheath elongation lasted until P7 (Figure 2I) and lacunae were visible at P6 (Figures 2D and 2I). The downregulation of *OSH1* was observed in the presumptive P0 region but not in the presumptive P1 region (Figure 2B). Accordingly, *pla2-1* leaves undergo a normal sequence of cell/tissue differentiation. However, since the duration of each PN stage is much shorter in *pla2-1* (1.8 d) than in the wild type (5.0 d), these results indicate that *pla2-1* leaves mature in a shorter time than wild-type leaves (i.e., *pla2-1* leaves mature in just 12.6 d compared with 30 d for wild-type leaves). Therefore, we can conclude that leaf maturation is accelerated in *pla2* (Figure 2I). This suggests that *PLA2* not only inhibits leaf initiation but also suppresses the progression of programs associated with leaf development.

SAM

Since leaves are initiated on the flank of the SAM, abnormal leaf initiation might be linked to SAM abnormalities. The SAM of *pla2* is much larger than that of the wild type (Figures 3A and 3B, Table 1); however, the shape of the SAM, represented by the ratio of the height to the width, was comparable among *pla2*, *pla1*, and the wild type (Table 1). Next, to gain insight into whether abnormal leaf initiation was associated with changes in cell division, we performed in situ hybridization experiments with the rice histone *H4* gene, which is specifically expressed in the S phase of the cell cycle. The *pla2-1* SAM showed an increase in the mean number of cells expressing histone *H4* per median longitudinal section of SAM (3.8 in *pla2-1* versus 0.7 in the wild type; Figures 3D and 3E, Table 1). This shows that SAM of *pla2* has a higher rate of cell division than the wild type, which could compensate for the rapid production of leaf primordia. *pla1-4* has an even larger SAM than *pla2-2* (Table 1), but the cell division activity was lower than that of *pla2-2* (Table 1). This indicates that shortened plastochron is more closely correlated with increased cell divisions than increases in SAM size.

Internode Elongation

In rice, only the upper four or five internodes elongate substantially at around the vegetative–reproductive transition. Internodes are designated as follows: the internode just below the uppermost one is designated the -1 internode, and the third, fourth, and fifth internodes counted from the top are -2, -3, and -4, respectively (Sunohara et al., 2003). Normally, internode length decreases basipetally in a geometric ratio (i.e., each internode is normally approximately twice as long as the next lower one) (Figures 4A and 4B). Both *pla2-1* and *pla2-2* mutants were extremely short (<10% of wild-type plant height) and showed an increased number and abnormal pattern of elongated

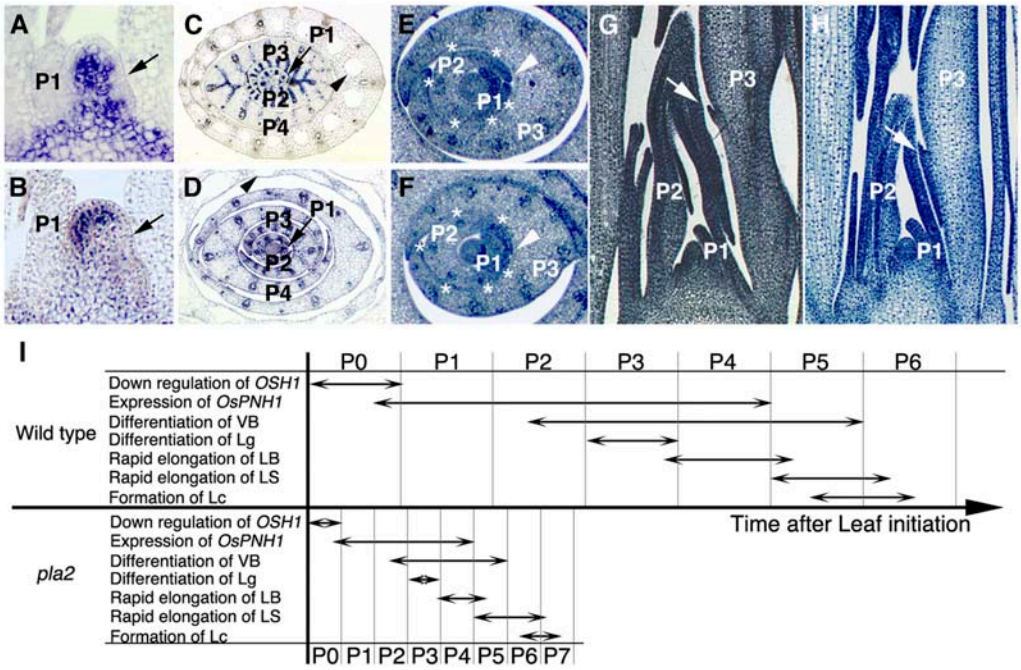

Figure 2. Accelerated Leaf Development in *pla2* Plants.

(A), **(C)**, **(E)**, and **(G)** The wild type.
(B), **(D)**, **(F)**, and **(H)** *pla2-1*.
(A) and **(B)** Expression of *OSH1* in the shoot apex. Downregulation of *OSH1* is observed in P0 (arrows).
(C) and **(D)** Expression of Os *PNH1* in the shoot apex. The arrows indicate the expression in P1. Lacuna formation is observed in the leaf sheath of P5 in the wild type and P6 in *pla2-1* (arrowheads).
(E) and **(F)** Cross section of shoot apex. Asterisks indicate differentiating procambial strands. The margins of the P2 sheath are overlapping (arrowheads).
(G) and **(H)** Longitudinal sections of the shoot apex. Arrows indicate the protrusion of ligule primordium.
(I) Schematic representation of the leaf developmental programs in the wild type and *pla2*. VB, vascular bundle; Lg, ligule; LB, leaf blade; LS, leaf sheath; Lc, lacuna.

internodes (Figures 4A and 4B). In both *pla2-1* and *pla2-2*, elongation was observed up to the -6 internode, but the uppermost internode did not show substantial elongation (Figures 4C and 4D). Although the geometric pattern of internode elongation was roughly conserved in *pla2* (except the uppermost one), the length of each internode was reduced (Figures 4A and 4B). The increase in the number of elongated internodes and the concomitant reduction of each internode length are reminiscent of events occurring in leaves: the increase in the number of leaves and the reduction of leaf size.

The cells of the internodes are somewhat smaller in *pla2* than in the wild type (see Supplemental Figure 3 online). By contrast, the number of cells in *pla2* internodes was significantly reduced. However, as *PLA2* is not expressed in stem (Figure 6C), shortened internodes would not be a direct effect of *pla2* mutation but a secondary effect of shortened leaves.

The *pla1* mutants showed different internode elongation patterns from *pla2* and, while dwarf, were significantly taller than *pla2* (Figure 4A). Substantial elongation occurred until the -8 internode, but the internode lengths were not in a geometric ratio (Figures 4A and 4B). Frequently, a lower internode was longer than higher ones. The uppermost internode did not elongate in the strong allele *pla1-4* (Figure 4E) and elongated only slightly in the mild allele *pla1-3*. Occasionally some internodes did not elongate, while immediately adjacent upper and lower ones did (Figure 4F).

Inflorescences

After the vegetative–reproductive transition, the rachis meristem of the wild type differentiates bracts (small leaf-like organs associated with floral branches) and branch primordia in 2/5 spiral manner (Figure 4H) and eventually aborts. Normally, bracts remain rudimentary, while the primary rachis branches produce secondary rachis branches and spikelets. In *pla2*, the reproductive phase starts almost normally, as judged from the formation of flag leaf (the last vegetative leaf morphologically distinguished from other leaves) and bracts. The *pla2* inflorescence, however, produced several vegetative shoots with enlarged bracts (Figure 4G) instead of primary branches. A close examination of a young *pla2* inflorescence revealed that primary branch primordia were initiated normally in spiral phyllotaxy (Figure 4I) but that several

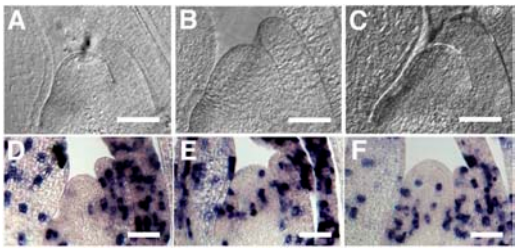

Figure 3. SAM and Histone *H4* Expression in Wild-Type, *pla2*, and *pla1* Plants at 3 Weeks after Germination.

(A) and **(D)** The wild type.
(B) and **(E)** *pla2-1.*
(C) and **(F)** *pla1-4*.
(A) to **(C)** Cleared image of SAMs.
(D) to **(F)** Expression of histone *H4*.
Bars = 50 μm.

proximal primordia were converted to vegetative shoots (Figure 4J), while more distal primordia aborted. These phenotypes resemble those of *pla1* (Figures 4G and 4K) and can be interpreted to result from a failure of certain elements of the vegetative program to terminate properly, leading to their coexpression with reproductive programs of development.

Identification of the *PLA2* Gene

To investigate the molecular function of *PLA2*, we isolated the *PLA2* gene by a map-based cloning strategy. The *PLA2* locus is closely linked with the marker R3202 on chromosome 1. Further fine mapping confined the *PLA2* locus to a 66-kb region in the P1 artificial chromosome clone P0497A05. This region was predicted to contain nine genes by an annotated rice gene database. Genome sequencing revealed that two independent *pla2* alleles had mutations in a putative gene designated P0497A05.11, comprising six exons and five introns (Figure 5A). In *pla2-1*, a C-to-T single base change causes Pro-to-Leu amino acid substitution in the sixth exon (Figure 5A). In *pla2-2*, a C-to-T single base change generates a stop codon in the first exon. To clarify whether the candidate gene represented *PLA2*, we performed a complementation test by introducing a 7.2-kb genomic fragment containing the candidate gene into *pla2-2* homozygous plant. As this fragment rescued the mutant phenotypes (see Supplemental Figure 4 online), we concluded that P0497A05.11 is *PLA2.* We did not observe any additional phenotype in the rescued plants.

The predicted PLA2 protein contains three RNA recognition motifs (RRM1, RRM2, and RRM3) and shows high similarity to the maize TE1 and the fission yeast MEI2 proteins (Figures 5B and 5C). The amino acid identities between PLA2 and TE1 in the three RRMs were 75.4, 74.6, and 89.5%, respectively, and those between PLA2 and MEI2 were 24.6, 29.9, and 52.6%, respectively (Figures 5B and 5C).

Anderson et al. (2004) have reported six MEI2-like proteins in rice and nine in *Arabidopsis* and divided them into two subfamilies: a MEI2-like subfamily and a TE1-like subfamily. PLA2 is identical to OML1 of the TE1-like subfamily. By BLAST search, we have identified an additional MEI2-like protein in rice, OML7, which like OML6, has only the C-terminal RRM. A phylogenetic tree based on a comparison of the highly conserved RRM3 domain indicates that PLA2 is likely to be the orthologue of TE1 (Figure 5D; see Supplemental Figure 5 online).

Expression of the *PLA2* Gene

To gain more insight into the biological function of *PLA2*, we examined the *PLA2* expression in detail. We first examined *PLA2* expression by RT-PCR analysis. RNA was isolated from 3-week-old vegetative shoot apices, the inflorescence apex, the leaf blade, the leaf sheath, and the root. *PLA2* was strongly expressed in shoot apex and inflorescence apex and intermediately in root, while low expression was detected in leaf blade and leaf sheath (see Supplemental Figure 6 online).

To obtain more detailed information on the spatial pattern of *PLA2* expression, we performed in situ hybridization experiments. By this method, *PLA2* expression was seen throughout the life cycle. In the embryo, transcripts were detected in leaf primordia, vascular bundles, and the radicle (Figure 6A). In the vegetative phase, *PLA2* was expressed in crown root apices (Figure 6B) and shoot apices (Figures 6C to 6F). Although Paquet et al. (2005) reported that *PLA2*/*Ostel1*/*OML1* was expressed in shoot apices but not in roots and leaves, we detected obvious expression in roots, though no mutant phenotypes were apparent in this organ. In the shoot apex, *PLA2* expression was first detected in the entire early P1 primordium that later developed into midrib (Figure 6C) and then became extended to the marginal region (Figure 6C). In P2-P4 primordia, the expression was localized to marginal and distal regions and was then downregulated from basal midrib region (Figures 6D to 6F). In older leaves than P4, *PLA2* transcripts could not be detected. Almost no or only low levels of *PLA2* transcripts could be detected in the SAM (Figure 6C). In the early reproductive phase, *PLA2* was expressed in bracts and several external layers of the rachis meristem (Figure 6G), suggesting that at this stage, *PLA2* may regulate meristem identity directly. At the later stages, *PLA2* was expressed in branch meristems, floral meristems, and floral

Table 1. Phenotypes of the Wild Type, *pla2*, and *pla1* in Vegetative Phase

	Taichung 65	*pla2-1*	*pla2-2*	*pla1-3*	*pla1-4*
Plastochron	5.0 ± 0.0	1.8 ± 0.0	1.8 ± 0.0	3.1 ± 0.1	2.3 ± 0.1
SAM width (A) (μm)	62.9 ± 5.8	77.0 ± 8.8	72.5 ± 5.5	69.5 ± 4.0	73.5 ± 3.1
SAM height (B) (μm)	34.1 ± 3.0	43.1 ± 8.2	39.9 ± 4.1	36.9 ± 3.9	40.6 ± 3.2
SAM shape (B/A)	0.54 ± 0.04	0.56 ± 0.07	0.55 ± 0.03	0.53 ± 0.04	0.55 ± 0.05

Values indicate the means of 20 experiments ± SD.

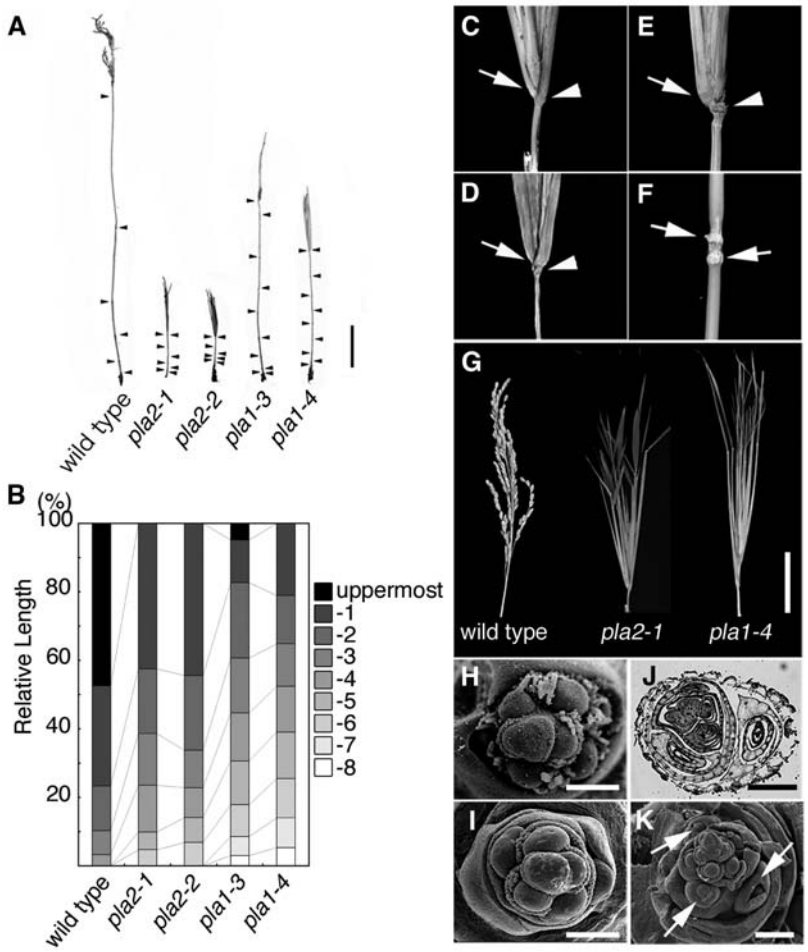

Figure 4. Reproductive Phenotypes of Wild-Type, *pla2*, and *pla1* Plants.

(A) Elongation pattern of internodes. The culm of the wild-type plant is longer than those of *pla* mutants. Arrowheads indicate nodes.
(B) Schematic representation of the elongation patterns of internodes in the wild type, *pla2-1*, *pla2-2*, *pla1-3*, and *pla1-4*.
(C) to **(E)** The nonelongating uppermost internodes of *pla2-1*, *pla2-2*, and *pla1-4*, respectively. Arrows indicate the neck nodes, and arrowheads indicate the flag leaf nodes. The flag leaf is removed in **(C)** and **(D)** to clarify the uppermost internode.
(F) Occasional nonelongation of internode in *pla1-4*. Arrows indicate two successive nodes.
(G) Inflorescences of the wild type, *pla2-1*, and *pla1-4* from left to right. In *pla2-1* and *pla1-4*, vegetative shoots emerge instead of primary branches.
(H) Scanning electron microscopy image of primary branch primordia in the wild type.
(I) Scanning electron microscopy image of primary branch primordia in *pla2-1*.
(J) Cross section of *pla2-1* young inflorescence showing ectopic shoots converted from primary branch primordia.
(K) Scanning electron microscopy image of primary branch primordia in *pla1-4*. Arrows indicate ectopic shoots.
Bars = 10 cm in **(A)**, 5 cm in **(G)**, 100 μm in **(H)**, **(I)**, and **(K)**, and 200 μm in **(J)**.

organs (Figures 6H and 6I). In the control experiment hybridized with sense RNA probe, no hybridization signals were detected (Figure 6J).

Relation between *PLA1* and *PLA2*

Although *PLA1* and *PLA2* encode unrelated proteins, a member of the P450 family and MEI2-like RNA binding protein, respectively, their loss-of-function mutants show very similar phenotypes. To understand how these genes are related, we assessed whether the expression and function of these genes is interdependent through expression analyses and comparisons of single versus double mutant phenotypes. In a *pla2-1* mutant, *PLA1* expression was localized normally in the basal abaxial region of young leaf primordia (Figures 7A and 7B). Conversely, *PLA2* expression was normal in *pla1-4* (Figures 7C and 7D). These results indicate that *PLA1* and *PLA2* are regulated independently of each other, suggesting that they function in independent pathways.

To elucidate genetic interaction, we made *pla1-2 pla2-1* double mutants. As was the case for single *pla1* and *pla2* mutants, no abnormalities were apparent in embryos of *pla1-2 pla2-1*. After germination, *pla1-2 pla2-1* initiated leaves more rapidly than

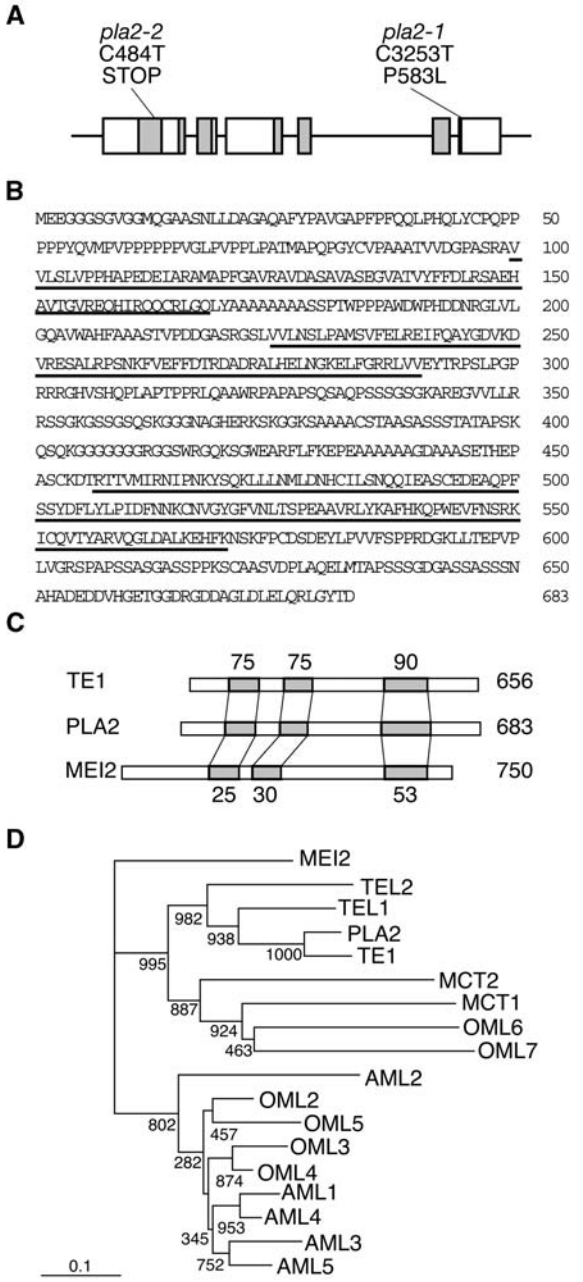

Figure 5. Structures of *PLA2* and Related Genes.

(A) Exon/intron structure of the *PLA2* gene. Six boxes indicate exons. RNA recognition motifs (RRMs) are shaded. Locations of the two *pla2* mutations are indicated: base and amino acid substitutions in exon 6 in *pla2-1* and base substitution and non-sense mutation in *pla2-2*.

(B) Deduced amino acid sequence of PLA2 protein. Underlining indicates RRMs.

(C) Comparison of PLA2, TE1, and MEI2 proteins. RRMs are shaded. Numbers above TE1 and below MEI2 represent amino acid identity between TE1 and PLA2 and MEI2 and PLA2, respectively. Numbers at the right side indicate the number of amino acids.

(D) Phylogenetic tree of MEI2-like RNA binding proteins. Numbers at each branch point indicate bootstrap values. PLA2, OML2, OML3, OML4, OML5, OML6, and OML7 are from *O. sativa*, TE1 from *Z. mays*, TEL1, TEL2, AML1, AML2, AML3, AML4, AML5, MCT1, and MCT2 from *Arabidopsis*, and MEI2 from *Schizosaccharomyces pombe*.

either single mutant (Figure 7E): the plastochron, 1.1 d, was much shorter than those of *pla1-2* (2.8 d) and *pla2-1* (1.8 d). The *pla1-2 pla2-1* SAM was larger than wild-type SAM but smaller than each single mutant SAM (data not shown). *pla1-2 pla2-1* also showed aberrant phyllotaxy. Cross sections revealed that in *pla1-2 pla2-1*, two successive leaf primordia were frequently formed on the same side of the SAM or with a divergence angle deviated from 180° (Figure 7F). In addition, two successive leaves could sometimes be seen fused on their margins (Figure 7F), probably due to an extremely short plastochron. None of the internodes in the double mutants showed substantial elongation (data not shown). In the reproductive phase, *pla1-2 pla2-1* produced many more ectopic shoots than *pla1-2* and *pla2-1* (Figure 7G), despite *pla1-2* being a weak allele that produces both normal inflorescence branches and a small number of ectopic shoots.

The independent regulation of gene expression and more severe phenotypes of the double mutants compared with the single mutants suggest that *PLA1* and *PLA2* act in the independent pathways that both contribute redundantly to the regulation of plastochron and the duration of vegetative phase.

Expression Profiles of *PLA2* and *te1* Differ

Since rice *PLA2* and maize *te1* are orthologous and loss-of-function mutants for both genes are available, it was of interest to make functional comparisons of these genes. With respect to gene expression, transcripts of both genes accumulate in the marginal and distal regions of young leaf primordia but appear downregulated in the basal central region (Figures 6C, 8A, and 8B; Veit et al., 1998). However, significant expression differences are observed in early stages of leaf development. *PLA2* transcripts are first observed in the central region of early P1 primordia and then extend toward the marginal region (Figure 6C), while *te1* is first expressed in semicircular bands whose arms include the incipient marginal region of P0 primordia but do not include the central region (Figures 8A and 8B; Veit et al., 1998). In summary, *te1* is expressed earlier than *PLA*2 (P0 versus P1); the expression extends from primordia margins to bracket the central region (in contrast with central-to-marginal progression in *PLA2*). A further difference in expression is observed in the reproductive phase, where strong *PLA2* expression is seen in bracts and inflorescence meristems (Figure 6G), in contrast with the *te1* inflorescence, where no transcripts were detected in RNA gel blot analysis (Veit et al., 1998). More recently, quite low levels of transcripts were detected in young tassel and ear only by a more sensitive competitive RT-PCR (D. Jeffares, unpublished data). These results suggest that *te1* expression is significantly lower during the reproductive phase than is seen for *PLA2*.

Mutant phenotypes also differ between *pla2* and *te1* mutants. While both *pla2* and *te1* initiate small leaves more rapidly than the wild type, the extent of plastochron reduction is larger in *pla2* (65%) than *te1* (35%) (Table 1; see Supplemental Table 1 online). The divergence angle between successive leaves in *pla2* is

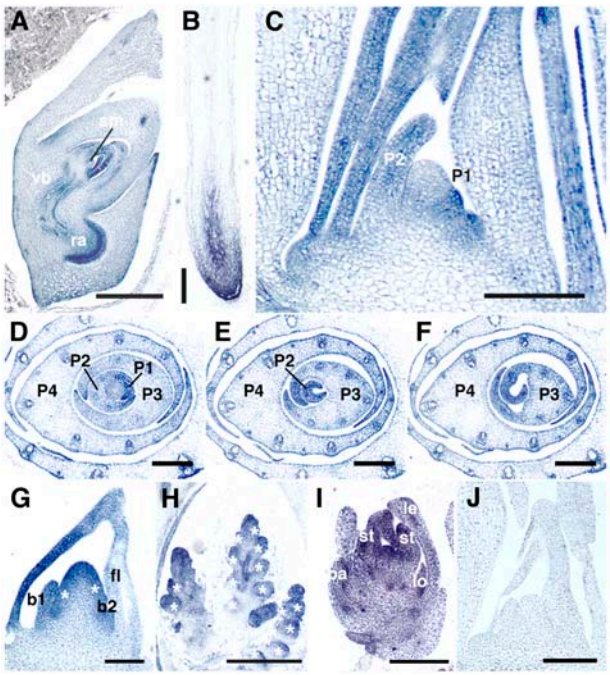

Figure 6. In Situ Localization of *PLA2* Transcripts.

(A) to **(I)** Antisense probe.
(J) Sense probe.
(A) Longitudinal section of embryo at 10 d after pollination. sm, SAM; vb, vascular bundle; ra, radicle.
(B) Crown root at 1 week after germination.
(C) Longitudinal section of 3-week-old shoot apex.
(D) to **(F)** Serial transverse sections of 3-week-old shoot apex. Panels are from the bottom to the top. *PLA2* signals are strong in marginal regions.
(G) Inflorescence apex at stage In2. Two primary rachis branches (asterisks) are formed. b1 and b2 indicate first and second bracts, respectively.
(H) Inflorescence apex at stage In5. Asterisks indicate spikelet primordia.
(I) Spikelet at stage Sp6. le, lemma; pa, palea; lo, lodicule; st, stamen.
(J) Longitudinal section of shoot apex. No hybridization signals are observed with sense probe.
Bars = 500 μm in **(A)**, 250 μm in **(B)** and **(H)**, 100 μm in **(C)**, **(G)**, and **(J)**, and 150 μm in **(D)** to **(F)** and **(I)**.

normal (180°) but is sometimes variable in *te1* (Veit et al., 1998). While *pla2* had large but normally shaped SAM, *te1* had a reduced misshapen SAM (Figures 8C and 8D; see Supplemental Table 1 online). Both mutants were dwarf but differed in internode elongation. Although dwarf, the relative pattern of internode elongation seen for *pla2* was nearly normal (Figure 4B), while *te1* showed irregular patterns of internode elongation (Veit et al., 1998). The most conspicuous differences were detected in the reproductive phase. Although both mutants developed large bracts (Figures 4G and 8E), the fates of subtended organs were quite different (Figures 4G and 8F). In *pla2*, primary branches were converted to vegetative shoots, while in *te1*, the normally male (stamen bearing) tassel branches were converted to female (kernel bearing) branches (Figure 8F). In some inbred backgrounds, this feminization was much less common (B. Veit, unpublished data).

DISCUSSION

In this article, we describe *pla2* mutants that show a combination of phenotypes related to the formation of leaves, including shortened plastochron, the reduction of leaf size due to precocious maturation, and the conversion of primary reproductive branches to vegetative shoots. While these phenotypes are very similar to those previously reported for *pla1* (Miyoshi et al., 2004), the results presented here suggest that the two genes normally function in distinct regulatory pathways. We show that *PLA2* encodes RNA binding protein that is unrelated to *PLA1*, a member of the P450 family. The transcriptional regulation of each gene is independent of the activity of the other. Finally, double mutants show synergistic phenotypes not seen in either single mutant. Taken together, these results provide support for a model in which the rate of leaf initiation, or plastochron, is directly coupled to the rate at which previously formed leaves mature.

PLA2 Encodes a MEI2-Like RNA Binding Protein

Our genetic and molecular analysis indicates that *PLA2* is the rice orthologue of *te1*, which like *PLA2*, encodes a MEI2-like RNA binding protein and shares a similar loss-of-function phenotype. MEI2-like proteins are named for their similarity to MEI2, which in *S. pombe* plays a crucial role in the transition to meiosis. Members of this family share a characteristic ribonucleoprotein-type RRM at their C terminus. In *S. pombe*, this RRM forms a complex with meiRNA, a noncoding RNA encoded by *SME2* locus (Watanabe and Yamamoto, 1994). The formation of this complex is essential for meiosis I but is not required for premeiotic DNA synthesis (Yamashita et al., 1998), which is thought to involve complexes with as yet undefined RNAs.

Although the high degree of conservation between the C-terminal RRMs of PLA2 and MEI2 suggested that they might bind similar target RNA(s), we could find nothing similar to *SME2* in rice. Other possible interactions remain to be tested. Recently, it was reported that signaling via small RNAs, such as small-interfering RNA and microRNA, is involved in many developmental processes in plants (Kidner and Martienssen, 2005), with some related to heterochrony (Bollman et al., 2003; Hunter et al., 2003; Achard et al., 2004; Peragine et al., 2004). This idea is supported by the result that overexpression of *miR156b* caused shortened plastochron in *Arabidopsis* (Schwab et al., 2005). Thus, it is possible that PLA2 binds to small RNAs and is involved in an RNA interference–mediated process. In any case, detection of the target RNAs of PLA2 should provide useful insights into molecular mechanisms of leaf development.

PLA2 Regulates the Rate of Leaf Maturation

Our analysis of the loss-of-function mutant phenotypes indicates that *PLA2* is a positive regulator of leaf size and a negative regulator of leaf initiation, although Paquet et al. (2005) have suggested, based on a more limited analysis of in situ hybridization data, that *PLA2*/*Ostel1*/*OML1* is a positive regulator of leaf initiation. Our analysis, however, shows that in the absence of *PLA2* function, small leaves develop as a result of precocious maturation (i.e., accelerated cell/tissue differentiation). Thus,

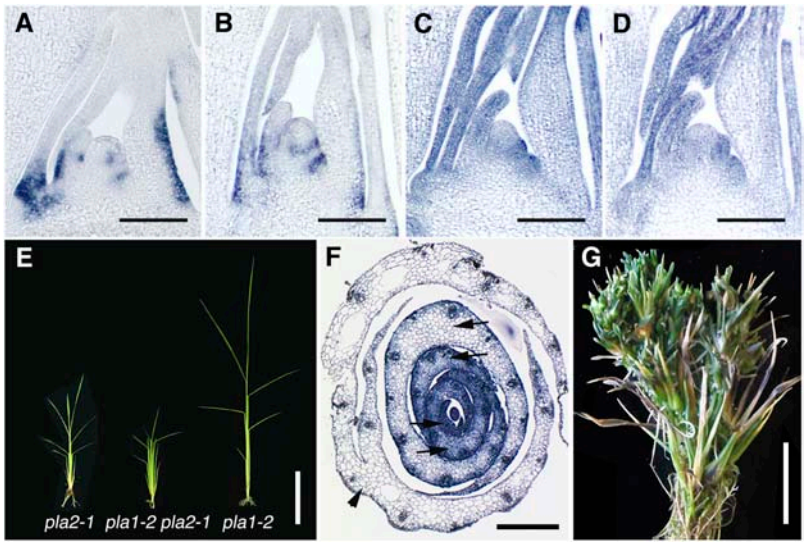

Figure 7. Relationship between *PLA1* and *PLA2*.

(A) Expression of *PLA1* in 1-month-old wild-type shoot apex.
(B) Expression of *PLA1* in *pla2-1* 1-month-old shoot apex.
(C) Expression of *PLA2* in 3-week-old shoot apex of the wild type.
(D) Expression of *PLA2* in 3-week-old shoot apex of *pla1-4*.
(E) Seedlings at 2 weeks after germination. *pla1-2 pla2-1* initiated more leaves than the *pla1-2* or *pla2-1* single mutant.
(F) Transverse sections of *pla1-2 pla2-1* shoot apex at 1 month after germination. Arrows indicate two successive leaves that are initiated from the same side of the SAM. Arrowhead indicates fusion of the margins of two successive leaves due to shortened plastochron.
(G) Inflorescence of *pla1-2 pla2-1*. *pla1-2 pla2-1* produced a large number of ectopic shoots (cf. with Figure 4G).
Bars = 100 μm in **(A)** to **(D)**, 5 cm in **(E)**, 200 μm in **(F)**, and 2.5 cm in **(G)**.

PLA2 would normally negatively regulate the rate of leaf maturation. This regulation of leaf maturation could be viewed as the primary function of *PLA2*, considering that *PLA2* expression is predominantly localized to leaf primordia (Figure 6). In this respect, a positive correlation between leaf size and plastochron is suggestive. We propose that the shortened plastochron of *pla2* is an indirect consequence of precocious leaf maturation and, as such, resembles *pla1*, which shows similar phenotypes and which is also expressed in leaf primordia but not in the SAM (Itoh et al., 1998; Miyoshi et al., 2004). In summary, analyses of *pla2* and *pla1* provide two independent examples that suggest that the rate of leaf maturation plays a significant role in regulating the rate of leaf initiation.

It is significant that expression domains in leaf primordia differ between *PLA2* and *PLA1*. *PLA2* is expressed strongly in marginal and distal regions (Figure 6), whereas *PLA1* expression is observed in the proximal abaxial region (Miyoshi et al., 2004). It is known that leaf maturation proceeds from the distal to proximal region (Freeling, 1992; Muehlbauer et al., 1997). Thus, *PLA2* may be involved in the maturation of distal tissues, while *PLA1* is more involved in maturation of proximal tissues. Since *pla1 pla2* double mutants exhibit much shorter plastochron than either mutant, *PLA2* and *PLA1* appear to have complementary functions in leaf maturation that together exert a strong effect on leaf plastochron.

It remains unclear how leaf maturation could affect plastochron. To date, almost no studies have focused specifically on the temporal regulation of leaf initiation but instead have considered factors that influence spatial regulation to give a characteristic leaf arrangement, or phyllotaxy. Several types of models have been proposed to explain this patterning, including the inhibitor, biophysical, and auxin transport models (Green, 1985; Steeves and Sussex, 1989; Reinhardt et al., 2003). Although the proposed mechanisms differ between models, they all maintain that young leaf primordia inhibit new primordium formation in a proximity-dependent manner. We propose that these schemes may also explain temporal regulation of leaf initiation (i.e., preexisting leaf primordia inhibit the precocious initiation of the next leaf). Based on data presented here, in which the precocious maturation of *pla2* and *pla1* leaves is associated with a reduced plastochron, we propose a model that explains how *PLA2* regulates plastochron (Figure 9). In this model, we postulate that leaves lose their inhibitory activity as they mature. Thus, in *pla2*, the inhibitory activity rapidly declines due to precocious maturation, resulting in more rapid leaf initiation. It remains for future study to determine the nature of this inhibitory signal and to understand its relationship to leaf maturation.

PLA2 Ensures Normal Termination of Vegetative Development

Both *pla2* and *pla1* show heterochronic traits, including the delayed transition to reproductive phase and conversion of rachis branches to vegetative shoots, suggesting that these

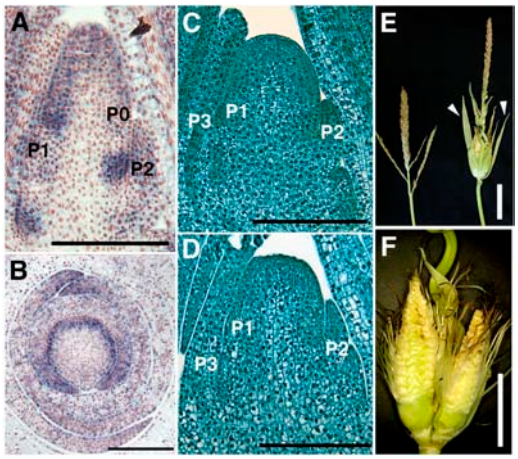

Figure 8. Phenotypes of *te1*.

(A) In situ localization of *te1* transcripts in longitudinal section of late vegetative shoot apex.
(B) In situ localization of *te1* transcripts in transverse section of late vegetative shoot apex.
(C) Wild-type shoot apex.
(D) *te1* shoot apex.
(E) Tassels of the wild type (right) and *te1* (left). Arrowheads indicate elongated husk leaves.
(F) Enlarged view of ectopic ears in the tassel of *te1*. Husk leaves are removed.
Bars = 200 μm in **(A)** to **(D)**, 5 cm in **(E)**, and 2.5 cm in **(F)**.

genes are required for normal termination of the vegetative phase. In maize, dominant heterochronic mutants *Teopod1* (*Tp1*), *Tp2*, and *Tp3* show a similar phenotype (Poethig, 1988; Dudley and Poethig, 1991, 1993; Bassiri et al., 1992) in which branches of tassel are converted into shoots. The *viviparous8* (*vp8*) mutations enhance the conversion in *Tp1*, *Tp2*, and *Tp3* backgrounds, although *vp8* never produces tassel shoots by itself (Evans and Poethig, 1997). Since these maize genes would have different molecular functions from *PLA2*, many genes appear to be involved in the termination of the vegetative program. Interestingly, *vp8* mutants show shortened plastochron, although *Tp* mutants do not. This suggests that *vp8* may play a similar role as *PLA1* and *PLA2*. As *Tp* mutants are dominant, *tp* genes may positively regulate vegetative programs. Unfortunately, these maize genes have not been cloned, and we do not have orthologous mutants in rice. However, one expectation is that *tp* homologues of rice are negatively regulated by *PLA2*, and they are expressed ectopically in the *pla2* mutant, where they promote the ectopic expression of vegetative programs.

A failure in the normal termination of the vegetative phase in *pla2* and *pla1* might also account for overgrowth of bracts that normally remain vestigial (Figure 4; Itoh et al., 1998), a phenotype that is also seen in *Tp* mutants of maize. Since both *PLA2* and *PLA1* are expressed strongly in bracts (Figure 6; Miyoshi et al., 2004), it is natural to speculate that normal bracts suppress the expression of the vegetative program in inflorescence. In the absence of *PLA2* or *PLA1* activity, bracts might adopt a pattern of development more similar to the much larger vegetative leaf. While vegetative leaves would mature more rapidly in the absence of *PLA* activity, they would still attain a larger size than normal bracts.

In contrast with *PLA1*, which is expressed only in bracts, *PLA2* is expressed in the upper region of the inflorescence meristem and branch meristems as well as in bracts. This indicates that *PLA2* may have some functions in addition to the inhibition of bract development. The inflorescence phenotype, however, does not differ between *pla2* and *pla1* except for the severity. It is reported that some *MEI2*-like genes in *Arabidopsis* are expressed in inflorescence meristems (Anderson et al., 2004). It may be that *MEI2* homologue(s) other than *PLA2* in rice are expressed in inflorescence meristems, where they function redundantly.

Plastochron Is More Closely Correlated to Cell Division Than SAM Size

We have already reported that for *pla1*, a shortened plastochron is correlated with an enlargement of the SAM and an increased frequency of cell divisions (Itoh et al., 1998). Our observations on *pla2* offer further support for this correlation but suggest that SAM size may be less significant. For example, although the SAM of *pla2-2* is not as large as that of *pla1-4*, it has a shorter plastochron. Similarly, the SAM of the *pla1-2 pla2-1* double mutant, which has a smaller SAM than either single mutant, has the shortest plastochron. The maize equivalent of *pla2*, *te1*, also shows a reduced SAM compared with the wild type but also has a shortened plastochron. Ikeda et al. (2005) have recently reported that *aberrant panicle organization1* of rice shows slightly shortened plastochron, but the SAM size is not modified. By contrast, Cockcroft et al. (2000) reported that higher cell division activity associated with constitutive expression of *cyclin* D in tobacco shortened plastochron without altering the SAM size. These results suggest that a reduced plastochron is more tightly linked to higher rates of cell division than to an increase in the size of the SAM. However, it should be noted that since no or only low levels of *PLA1* and *PLA2* transcripts are observed in SAM, their effects on cell divisions in the SAM are likely to be indirect. We

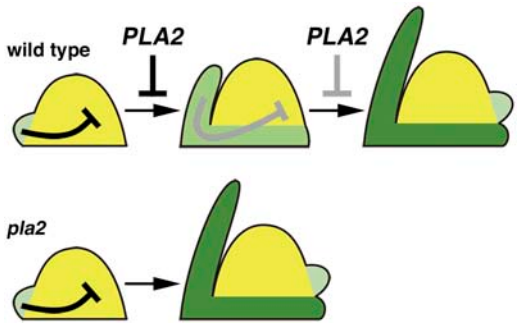

Figure 9. Model of Plastochron Regulation.

Leaf initiation is inhibited by the preexisting immature leaf primordia. *PLA2* limits the rate of leaf development; as leaf development proceeds, the inhibitory effect becomes weakened and finally allows the next leaf to be initiated. In *pla2*, leaves mature precociously, and the inhibitory effect is cancelled sooner than in the wild type.

propose that precocious maturation of leaves leads to a premature reduction of signal(s) that normally limits cell division in the SAM.

Functional Diversification of *PLA2*-Like Activities

In addition to delaying the maturation of leaves, *PLA2* and closely related genes appear to encompass additional activities as deduced from phenotypic differences. These differences could be explained in several ways. One explanation would suppose that the genes regulate distinct downstream targets either by complexing with distinct target RNAs or, alternatively, through the formation of similar complexes that activate distinct pathways in maize and rice. A second explanation would attribute functional differences to the overlapping but nonidentical expression patterns of the two genes. Such expression differences have been described among several *FLORICAULA* (*FLO*)/*LEAFY* (*LFY*) orthologues in grasses, including rice *RFL*, maize *Zea FLO/LFY1* (*zfl1*) and *zfl2*, and *Lolium temlentum LFY* (Kyozuka et al., 1998; Gocal et al., 2001; Bomblies et al., 2003), and may be responsible for clear differences in the inflorescence architecture between these species.

Our analysis of expression differences seen for *PLA2*-like genes might largely account for changes in apparent activity during development and between species. During vegetative development, both *PLA2* and *te1* affect plastochron, with both genes normally acting to extend plastochron. However, the reduction of plastochron associated with loss of function is relatively modest in *te1* compared with *pla2.* More obvious differences are associated with the SAM, which is reduced and misshapen in *te1* compared with the enlarged but relatively normal shaped SAM of *pla2.* Finally, the extent to which internode development is affected differs, with more shortened internodes observed in the *te1* mutant. We propose that all of these differences can be related to observed differences in expression between the *PLA2* versus *te1* gene, where the ratio of expression in the SAM versus leaf is significantly higher for *te1.* By this model, *PLA2*-like genes would act to delay maturation processes not just in developing leaves, but in other tissues in which they are expressed. Higher expression of *te1* in the SAM would promote proliferation of cells and thus enhance the sizes of the SAM and associated internodes. A broader activity for *PLA2*-like genes is also supported by the expression patterns of related genes in *Arabidopsis*, which are specifically expressed in the apical meristem regions of the shoot and root that contain pluripotent stem cells (Anderson et al., 2004).

During reproductive development, the relatively strong expression of *PLA2* compared with *te1* correlates well with differences in mutant phenotypes. During this phase, *pla2* mutants form vegetative branches bearing normal leaves in place of inflorescence branches. By contrast, relatively minor changes are seen in *te1* mutants, where some feminization of basal branches is seen. Other aspects of inflorescence development are relatively normal, including the formation of a relatively dense array of floral branches. Thus, it would appear that expression differences can largely account for the functional diversification between *PLA2* and *te1*.

In this article, we have documented a clear role for *PLA2* in regulating the maturation of leaf primordia that in turn is clearly linked to the processes that regulate the formation of new leaves. Our molecular characterization of *PLA2* indicates that it effects this regulation through an RNA binding protein that is expressed in young leaf primordia. Thus, the primary function of *PLA2* is to regulate the rate of leaf maturation. *PLA2* also has an important function in the suppression of the vegetative program in the reproductive phase. Our analysis also provides key insights into the nature of signals that regulate the initiation of leaves. Although previous studies have shown that leaf initiation can be inhibited by preexisting leaves in a proximity-dependent fashion, our study shows that the maturation state of the leaf would have a strong influence on this inhibition. Further analyses focused on the nature of these maturation-dependent signals should afford valuable insights into the regulation of plant development.

METHODS

Plants and Plastochron Measurement

We identified two single-gene recessive mutants from an M2 population of rice (*Oryza sativa*) cv Taichung 65 mutagenized with *N*-methyl-*N*-nitrosourea that showed a short plastochron like *pla1*. Allelism test revealed that the two mutants, designated *pla2-1* and *pla2-2*, were allelic to each other but distinct from *PLA1*. We also used *pla1-3* and *pla1-4* mutants derived from cv Taichung 65 (Miyoshi et al., 2004). *pla1-4* is the most severe allele among four *pla1* alleles. Mutant and wild-type plants were grown in pots or in paddy fields under natural conditions. Transgenic plants were grown in a biohazard greenhouse at 30°C in the day and 25°C at night.

When every new leaf blade had emerged completely from the sheath of the previous leaf, five plants at the same developmental stage were sampled, and the number of leaves was counted for each plant. At any stage of the vegetative phase, the number of immature leaves before emergence was nearly constant in both *pla2* and *pla1* (four or five leaves) and wild-type plants (three or four leaves). This indicates that leaf emergence rate corresponds to leaf initiation rate. Thus, we consider that leaf emergence rate is equal to leaf initiation rate (plastochron).

For generating double mutants between *pla1* and *pla2*, we crossed *PLA1-2/pla1-2* heterozygous plants with pollen of *PLA2-1/pla2-1. pla1-2 pla2-1* plants were identified by phenotypic characterization and molecular genotyping.

Developmental stages of rice inflorescence were represented according to the system of Ikeda et al. (2004).

The standard reference allele *te1-1* that had been introgressed into a B73 background that had been grown under standard field conditions was used for comparisons with maize (*Zea mays*).

Paraffin Sectioning and SAM Measurement

Shoot apices of the wild type and *pla2* were fixed in FAA (formaldehyde: glacial acetic acid:ethanol [1:1:18]) for 24 h at 4°C and then dehydrated in a graded ethanol series. Dehydrated samples in 100% ethanol were replaced with xylene and embedded in Paraplast plus (Oxford Labware). Microtome sections (8 μm thick) were stained with Delafield's hematoxyline and observed with a light microscope. For measurement of SAM sizes, dehydrated shoot apices were cleared in the benzyl-benzoate-four-and-a-half fluid devised by Herr (1982). Cleared shoot apices were observed with a microscope (IMT-2; Olympus) equipped with Nomarski differential interference contrast optics. The width of the

shoot apex was measured just above the P1 leaf primordium insertion, and the height of the shoot apex was given as the shortest distance from the line used for measuring the width to the tip of the apex.

For maize, shoot apices were infiltrated and sectioned as described by Jackson et al. (1994).

Scanning Electron Microscopy

Dehydrated samples in 100% ethanol were infiltrated with 3-methyl-butyl-acetate, critical point dried, sputter coated with platinum, and observed under a scanning electron microscope (S-4000; Hitachi) at an accelerating voltage of 10 kV.

In Situ Hybridization

Paraffin sections were prepared as described above except that 8-μm-thick microtome sections were applied to slide glasses coated with APS (Matsunami Glasses). Digoxigenin-labeled antisense and sense probes were prepared from the full-length cDNAs of histone *H4*, *PLA1*, and *PLA2*. In situ hybridization and immunological detection of the hybridization signals were performed as described by Kouchi and Hata (1993), except that hybridizations were performed at 55°C for *PLA1* and *PLA2* because of the high GC contents of these genes. For *te1*, in situ hybridization was performed as described by Jackson et al. (1994) except that hybridizations were performed at 60 to 65°C because of the high GC content.

RNA Isolation and Analysis

Total RNA was extracted from 100 mg of tissue (shoot apices, leaves, and inflorescence apices) using TRIZOL reagent (Invitrogen). After RNase-free DNase (Takara) treatment, 2.5 μg of RNA was reverse transcribed using oligo(dT) primer and SuperScript III (Invitrogen). PCR was performed for 30 cycles at 94°C for 45 s, 58°C for 30 s, and 72°C for 30 s using 5′-ACAAGGCGTTCCACAAGCAACC-3′ and 5′-GGCGCTGTCATGAG-CTCCTG-3′ for *PLA2* and 5′-TCCATCTTGGCATCTCTCAG-3′ and 5′-GTA-CCCGCATCAGGCATCTG-3′ for *ACTIN*.

Map-Based Cloning

F2 populations of *PLA2*/*pla2-1* (subsp *japonica*) and cv Kasalath (subsp *indica*) were used as mapping populations. Using multiple restriction fragment length polymorphism, sequence-tagged sites, and cleaved-amplified polymorphic sequence markers, the *PLA2* locus was confined to a 66-kb region on the P1 artificial chromosome clone P0497A05. For complementation tests, the 7.2-kb *Spe*I fragment, including the *PLA2* candidate and 1.8 kb direct upstream of initiation codon, was cloned into binary vector and introduced into *pla2-2* homozygotes by the *Agrobacterium tumefaciens*–mediated transformation method (Hiei et al., 1994).

Phylogenetic Analysis

Multiple sequence alignments were performed using ClustalX (Thompson et al., 1997) and BOXSHADE (http://searchlauncher.bcm.tmc.edu/multi-align/multi-align.html) programs. The phylogenetic tree was constructed based on the well-conserved RRM3 domain by the neighbor-joining method using ClustalX and TreeView (Page, 1996) programs. The numbers at the branching points indicate the times that each branch topology was found during bootstrap analysis ($n = 1000$).

Accession Numbers

Sequence data from this article can be found in the GenBank/EMBL data libraries under the following accession numbers: AB244276 to AB244282 (*PLA2* and *OML2* to *OML7*, respectively), CAA15822 (*MEI2*), AAK29419 (*te1*), NP_568946 (At5g61960, *AML1*), NP_973674 (At2g42890, *AML2*), NP_193546 (At4g18120, *AML3*), NP_196346 (At5g07290, *AML4*), NP_849727 (At1g29400, *AML5*), NP_189242 (At3g26120, *TEL1*), NP_176943 (At1g67770, *TEL2*), NP_174902 (At1g37140, *MCT1*), and NP_196410 (At5g07930, *MCT2*).

Supplemental Data

The following materials are available in the online version of this article.

Supplemental Figure 1. Boundary between Leaf Blade and Sheath.

Supplemental Figure 2. Changes of Leaf Size in Wild-Type, *pla2*, and *pla1* Plants.

Supplemental Figure 3. Epidermal Cells of the Third Leaves and Cells of -2 Internodes.

Supplemental Figure 4. Complementation Test of the *pla2* Mutation.

Supplemental Figure 5. Amino Acid Sequence Alignment of MEI2-Like Proteins, Which Are Used to Construct the Phylogenetic Tree.

Supplemental Figure 6. RT-PCR Analysis of the *PLA2* mRNA Expression in Different Tissues.

Supplemental Table 1. Plastochron and SAM in the Wild Type and *te1.*

ACKNOWLEDGMENTS

We thank Makoto Matsuoka (Nagoya University, Nagoya, Japan) for kindly providing *OSH1* and histone *H4* cDNA clones and Momoyo Ito and Kyoko Ikeda (University of Tokyo) for technical advice. We also thank Noboru Washizu, Ken-Ichiro Ichikawa, Shizue Nakata, and Hiroshi Kimura (University of Tokyo) for their assistance in cultivating rice plants at the Experimental Farm of the University of Tokyo. This work is supported in part by a Grant-in-Aid for Scientific Research from the Ministry of Education, Culture, Sports, Science, and Technology of Japan (14036206 and 16208002 to Y.N.) and by Marsden Fund grants to B.V.

Received September 1, 2005; revised December 13, 2005; accepted January 13, 2006; published February 3, 2006.

REFERENCES

Achard, P., Herr, A., Baulcombe, D.C., and Harberd, N.P. (2004). Modulation of floral development by a gibberellin-regulated microRNA. Development **131,** 3357–3365.

Anderson, G.H., Alvarez, N.D., Gilman, C., Jeffares, D.C., Trainor, V.C., Hanson, M.R., and Veit, B. (2004). Diversification of genes encoding mei2-like RNA binding proteins in plants. Plant Mol. Biol. **54,** 653–670.

Asai, K., Satoh, N., Sasaki, H., Satoh, H., and Nagato, Y. (2002). A rice heterochronic mutant, *mori1*, is defective in the juvenile-adult phase change. Development **129,** 265–273.

Bassiri, A., Irish, E.E., and Poethig, R.S. (1992). Heterochronic effects of *Teopod 2* on the growth and photosensitivity of the maize shoot. Plant Cell **4,** 497–504.

Bollman, K.M., Aukerman, M.J., Park, M.Y., Hunter, C., Berardini, T.Z., and Poethig, R.S. (2003). *HASTY*, the Arabidopsis ortholog of *exportin 5/MSN5*, regulates phase change and morphogenesis. Development **130,** 1493–1504.

Bomblies, K., Wang, R.L., Ambrose, B.A., Schmidt, R.J., Meeley, R.B., and Doebley, J. (2003). Duplicate *FLORICAULA/LEAFY* homologs *zfl1* and *zfl2* control inflorescence architecture and flower patterning in maize. Development **130,** 2385–2395.

Chaudhury, A.M., Letham, S., Craig, S., and Dennis, E.S. (1993). *amp1* - A mutant with high cytokinin levels and altered embryonic pattern, faster vegetative growth, constitutive photomorphogenesis and precocious flowering. Plant J. **4,** 907–916.

Cockcroft, C.E., den Boer, B.G., Healy, J.M., and Murray, J.A. (2000). Cyclin D control of growth rate in plants. Nature **405,** 575–579.

Dudley, M., and Poethig, R.S. (1991). The effect of a heterochronic mutation, *Teopod2*, on the cell lineage of the maize shoot. Development **111,** 733–739.

Dudley, M., and Poethig, R.S. (1993). The heterochronic *Teopod1* and *Teopod2* mutations of maize are expressed non-cell-autonomously. Genetics **133,** 389–399.

Evans, M.M.S., and Poethig, R.S. (1997). The *viviparous8* mutation delays vegetative phase change and accelerates the rate of seedling growth in maize. Plant J. **12,** 769–779.

Fleming, A.J., McQueen-Mason, S., Mandel, T., and Kuhlemeier, C. (1997). Induction of leaf primordia by the cell wall protein expansin. Science **276,** 1415–1418.

Freeling, M. (1992). A conceptual framework for maize leaf development. Dev. Biol. **153,** 44–58.

Giulini, A., Wang, J., and Jackson, D. (2004). Control of phyllotaxy by the cytokinin-inducible response regulator homologue *ABPHYL1.* Nature **430,** 1031–1034.

Gocal, G.F., King, R.W., Blundell, C.A., Schwartz, O.M., Andersen, C.H., and Weigel, D. (2001). Evolution of floral meristem identity genes. Analysis of *Lolium temulentum* genes related to *APETALA1* and *LEAFY* of Arabidopsis. Plant Physiol. **125,** 1788–1801.

Gould, S.J. (1977). Ontogeny and Phylogeny. (Cambridge, MA: Belknap Press of Harvard University Press).

Green, P.B. (1985). Surface of the shoot apex: A reinforcement-field theory for phyllotaxis. J. Cell Sci. Suppl. **2,** 181–201.

Helliwell, C.A., Chin-Atkins, A.N., Wilson, I.W., Chapple, R., Dennis, E.S., and Chaudhury, A. (2001). The Arabidopsis *AMP1* gene encodes a putative glutamate carboxypeptidase. Plant Cell **13,** 2115–2125.

Herr, J.M., Jr. (1982). An analysis of methods for permanently mounting ovules cleared in four-and-a-half type clearing fluids. Stain Technol. **57,** 161–169.

Hiei, Y., Ohta, S., Komari, T., and Kumashiro, T. (1994). Efficient transformation of rice (*Oryza sativa* L.) mediated by Agrobacterium and sequence analysis of the boundaries of the T-DNA. Plant J. **6,** 271–282.

Hunter, C., Sun, H., and Poethig, R.S. (2003). The Arabidopsis heterochronic gene *ZIPPY* is an *ARGONAUTE* family member. Curr. Biol. **13,** 1734–1739.

Ikeda, K., Nagasawa, N., and Nagato, Y. (2005). *ABERRANT PANICLE ORGANIZATION1* temporally regulates meristem identity in rice. Dev. Biol. **282,** 349–360.

Ikeda, K., Sunohara, H., and Nagato, Y. (2004). Developmental course of inflorescence and spikelet in rice. Breed. Sci. **54,** 147–156.

Itoh, J., Nonomura, K., Ikeda, K., Yamaki, S., Inukai, Y., Yamagishi, H., Kitano, H., and Nagato, Y. (2005). Rice plant development: From zygote to spikelet. Plant Cell Physiol. **46,** 23–47.

Itoh, J.I., Hasegawa, A., Kitano, H., and Nagato, Y. (1998). A recessive heterochronic mutation, *plastochron1*, shortens the plastochron and elongates the vegetative phase in rice. Plant Cell **10,** 1511–1522.

Jackson, D., and Hake, S. (1999). Control of phyllotaxy in maize by the *abphyl1* gene. Development **126,** 315–323.

Jackson, D., Veit, B., and Hake, S. (1994). Expression of maize *Knotted1* related homeobox genes in the shoot apical meristem predicts patterns of morphogenesis in the vegetative shoot. Development **120,** 405–413.

Kidner, C.A., and Martienssen, R.A. (2005). The developmental role of microRNA in plants. Curr. Opin. Plant Biol. **8,** 38–44.

Kouchi, H., and Hata, S. (1993). Isolation and characterization of novel nodulin cDNAs representing genes expressed at early stages of soybean nodule development. Mol. Gen. Genet. **238,** 106–119.

Kyozuka, J., Konishi, S., Nemoto, K., Izawa, T., and Shimamoto, K. (1998). Down-regulation of *RFL*, the *FLO/LFY* homolog of rice, accompanied with panicle branch initiation. Proc. Natl. Acad. Sci. USA **95,** 1979–1982.

Miyoshi, K., Ahn, B.O., Kawakatsu, T., Ito, Y., Itoh, J., Nagato, Y., and Kurata, N. (2004). *PLASTOCHRON1*, a timekeeper of leaf initiation in rice, encodes cytochrome P450. Proc. Natl. Acad. Sci. USA **101,** 875–880.

Muehlbauer, G.J., Fowler, J.E., and Freeling, M. (1997). Sectors expressing the homeobox gene *liguleless3* implicate a time-dependent mechanism for cell fate acquisition along the proximal-distal axis of the maize leaf. Development **124,** 5097–5106.

Nishimura, A., Ito, M., Kamiya, N., Sato, Y., and Matsuoka, M. (2002). *OsPNH1* regulates leaf development and maintenance of the shoot apical meristem in rice. Plant J. **30,** 189–201.

Page, R.D. (1996). TreeView: An application to display phylogenetic trees on personal computers. Comput. Appl. Biosci. **12,** 357–358.

Paquet, N., Bernadet, M., Morin, H., Traas, J., Dron, M., and Charon, C. (2005). Expression patterns of *TEL* genes in Poaceae suggest a conserved association with cell differentiation. J. Exp. Bot. **56,** 1605–1614.

Peragine, A., Yoshikawa, M., Wu, G., Albrecht, H.L., and Poethig, R.S. (2004). *SGS3* and *SGS2/SDE1/RDR6* are required for juvenile development and the production of trans-acting siRNAs in Arabidopsis. Genes Dev. **18,** 2368–2379.

Pien, S., Wyrzykowska, J., McQueen-Mason, S., Smart, C., and Fleming, A. (2001). Local expression of expansin induces the entire process of leaf development and modifies leaf shape. Proc. Natl. Acad. Sci. USA **98,** 11812–11817.

Poethig, R.S. (1988). Heterochronic mutations affecting shoot development in maize. Genetics **119,** 959–973.

Prigge, M.J., and Wagner, D.R. (2001). The *Arabidopsis serrate* gene encodes a zinc-finger protein required for normal shoot development. Plant Cell **13,** 1263–1279.

Reed, J.W., Nagpal, P., Poole, D.S., Furuya, M., and Chory, J. (1993). Mutations in the gene for the red/far-red light receptor phytochrome B alter cell elongation and physiological responses throughout Arabidopsis development. Plant Cell **5,** 147–157.

Reinhardt, D., Mandel, T., and Kuhlemeier, C. (2000). Auxin regulates the initiation and radial position of plant lateral organs. Plant Cell **12,** 507–518.

Reinhardt, D., Pesce, E.R., Stieger, P., Mandel, T., Baltensperger, K., Bennett, M., Traas, J., Friml, J., and Kuhlemeier, C. (2003). Regulation of phyllotaxis by polar auxin transport. Nature **426,** 255–260.

Sato, Y., Hong, S.K., Tagiri, A., Kitano, H., Yamamoto, N., Nagato, Y., and Matsuoka, M. (1996). A rice homeobox gene, *OSH1*, is expressed before organ differentiation in a specific region during early embryogenesis. Proc. Natl. Acad. Sci. USA **93,** 8117–8122.

Schwab, R., Palatnik, J.F., Riester, M., Schommer, C., Schmid, M., and Weigel, D. (2005). Specific effects of microRNAs on the plant transcriptome. Dev. Cell **8,** 517–527.

Snow, M., and Snow, R. (1931). Experiments on phyllotaxis. I. The effect of isolating a primordium. Philos. Trans. R. Soc. Lond. B **221,** 1–43.

Steeves, T.A., and Sussex, I.M. (1989). Patterns in Plant Development. (Cambridge, UK: Cambridge University Press).

Sunohara, H., Satoh, H., and Nagato, Y. (2003). Mutations in panicle development affect culm elongation in rice. Breed. Sci. **53,** 109–117.

Telfer, A., and Poethig, R.S. (1998). *HASTY*: A gene that regulates the timing of shoot maturation in *Arabidopsis thaliana.* Development **125,** 1889–1898.

Thompson, J.D., Gibson, T.J., Plewniak, F., Jeanmougin, F., and Higgins, D.G. (1997). The CLUSTAL_X windows interface: Flexible strategies for multiple sequence alignment aided by quality analysis tools. Nucleic Acids Res. **25,** 4876–4882.

Veit, B., Briggs, S.P., Schmidt, R.J., Yanofsky, M.F., and Hake, S. (1998). Regulation of leaf initiation by the *terminal ear 1* gene of maize. Nature **393,** 166–168.

Watanabe, Y., and Yamamoto, M. (1994). *S. pombe mei2*+ encodes an RNA-binding protein essential for premeiotic DNA synthesis and meiosis I, which cooperates with a novel RNA species meiRNA. Cell **78,** 487–498.

Yamashita, A., Watanabe, Y., Nukina, N., and Yamamoto, M. (1998). RNA-assisted nuclear transport of the meiotic regulator Mei2p in fission yeast. Cell **95,** 115–123.